Assessing HF radar capabilities to resolve mesoscale eddy interactions with littoral waters

Sylvia Rodríguez-Abudo*†§, Miguel Canals*†§, Julio Morell*‡§, Pedro Matos§, Carlos García§, Luis Pomales‡, and Jorge Capella§

*Center for Applied Ocean Sciences and Engineering University of Puerto Rico at Mayaguez, Mayaguez, Puerto Rico 00680
†Department of Engineering Sciences and Materials University of Puerto Rico at Mayaguez, Mayaguez, Puerto Rico 00680
‡Department of Marine Sciences University of Puerto Rico at Mayaguez, Mayaguez, Puerto Rico 00680
§IOOS Caribbean Coastal Ocean Observing System, Lajas, Puerto Rico 00677
Email: rodriguez.abudo@upr.edu (corresponding author)

***Abstract*—Eularian and lagrangian observations collected through the Caribbean Coastal Ocean Observing System (CARICOOS) and satellite imagery suggest that the interaction between mesoscale eddies (MSEs) and littoral waters may be significant in the southern coast of Puerto Rico (northern Caribbean Sea), where the insular shelf is narrow (O[10 km]); tidal ranges are low (<0.5 m), high swells are almost inexistent; nearshore bathymetry is complex; and MSE activity is high. A recent expansion of the CARICOOS HF Radar network allows for unprecedented coverage of near-surface currents near the southwestern coast of Puerto Rico, with the potential to detect and track such mesoscale ocean features. This study assesses the shoreward extent at which CARICOOS HF radars are able to resolve near-surface currents potentially resulting from mesoscale forcings. The approach taken consists of time and frequency domain comparisons of HF radial velocities (ideal and measured) with a moored ADCP, as well as qualitative comparisons with drifter trajectories. Potential implications of this work include: 1) implementation on ecological early warnings systems; 2) navigational safety and optimization; 3) fisheries management; among others.**

I. Introduction

Our physical, chemical, and biological understanding of the three-dimensional structure of mesoscale eddies (MSEs) in the deep ocean and shelf break has been significantly increased over the past decades. Numerous remote (see [1] for a review), in situ (e.g. [2]), and laboratory (e.g. [3]) observations have well served this purpose and have provided useful information for large scale ocean circulation models. While MSEs not often make it shoreward of the continental shelf due to their low Rossby number, it is well documented that they can interact with the shelf system (e.g. [4]). Closer to shore, mesoscale forcings are usually neglected in the littoral momentum balance, perhaps because their temporal and spatial scales significantly differ from those of the relevant littoral hydrodynamics.

Nearshore data from the Caribbean Coastal Ocean Observing System (CariCOOS) suggest that the interaction between MSEs and littoral waters are rather substantial in the southern coast of Puerto Rico, which is characterized by a narrow insular shelf (O[10 km]); low tidal ranges (<0.5 m) and swells, complex nearshore bathymetry; and high MSE activity. For example, complex structures resulting from the MSE's boundary shear instabilities are often times revealed in satellite imagery of suspended matter advected from the littoral zone (see for example ESA's EnviSAT MERIS sensor image for 09/19/05, available at `http:\\images.caricoos.org\Archive_MERIS_TSM_FINAL\`). Very recent Lagrangian observations collected as part of the CariCOOS-Caribbean Fisheries Management Council drifter program clearly evidence shelf waters from Puerto Rico west and south coasts diverted into a mesoscale structure located south of the Mona Passage (Figure 1, [5]). Moreover, qualitative comparisons between shelf currents measured by the CariCOOS PR108 buoy and those derived from satellite altimetry more than 5 km off the shelf break, reveal a strong linkage in the hydrodynamics, even at fairly different geostrophic conditions (Figure 2).

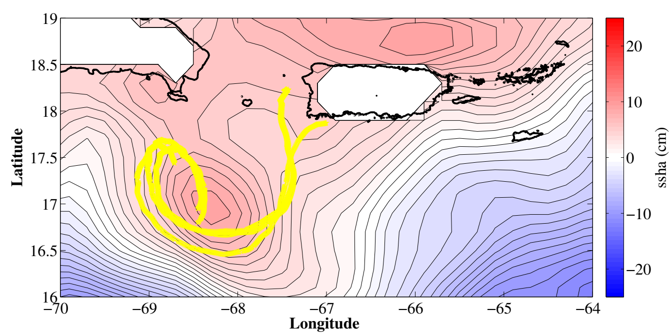

Fig. 1. Drifter trajectories for March 15-30, 2015 (yellow) over contours of average sea surface height anomaly for the same period.

While moored data from CariCOOS buoys provide valuable insight into littoral hydrodynamics, they are only able to resolve near-surface velocities at a point. To this end, CariCOOS' new HF radar expansion aims at providing unprecedented coverage of near-surface current data for the southwestern coast of Puerto Rico. Since February 2015 a pair of long-range antennas located in Cabo Rojo and Ponce resolve near-surface currents on an hourly basis. With the overarching goal of achieving sufficient coverage to study MSE interactions with littoral waters, this paper explores the

This is a DRAFT. As such it may not be cited in other works. The citable Proceedings of the Conference will be published in IEEE Xplore shortly after the conclusion of the conference.

978-0-933957-43-5 ©2015 MTS

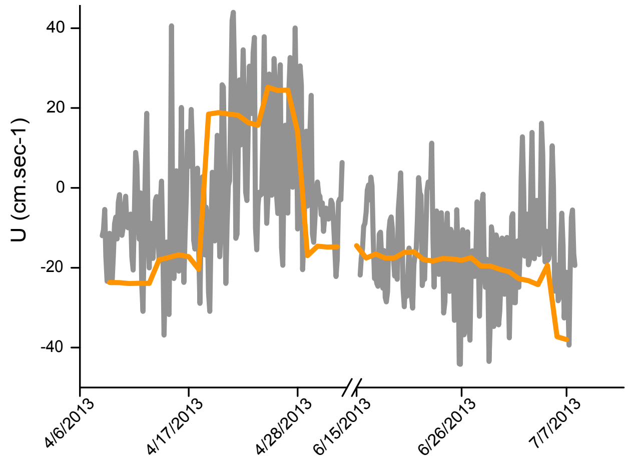

Fig. 2. Easting velocities as measured by CariCOOS PR108 buoy (gray) and NOAA's Coastwatch Geostrophic product (orange).

shoreward extent at which CariCOOS HF radars are able to accurately and reliably resolve near-surface currents in the littoral zone.

II. Observations

A. Site description

The study site is located off the southern coast of Puerto Rico (northern Caribbean Sea, Figure 3), where the continental shelf fluctuates between 7 and 20 km wide. The K1 (diurnal) constituent dominates the tidal signal in this region, with a maximum range of 0.21 m. During the validation experiment, surface currents were predominantly directed westwards and rarely exceeded 30 cm s^{-1} (Figures 4b-c). Similarly, trade winds averaging 8 m s^{-1} dominated the meteorological forcing (Figures 4d-e). Significant wave heights did not exceed 2 m, while dominant wave period remained roughly at 7 seconds (Figure 4f-g).

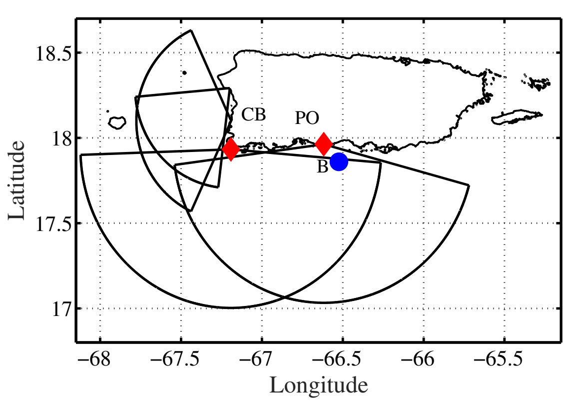

Fig. 3. CariCOOS HF radar network and associated coverage. Red diamonds represent the location of the Cabo Rojo (CB) and Ponce (PO) antennas, while the blue circle depict the location of the CariCOOS PR108 buoy.

B. HF radars

Hourly near-surface current data near the southwestern coast of Puerto Rico were provided by two long-range CODAR SeaSonde stations, part of the CariCOOS HF radar network, located in Cabo Rojo (CB) and Ponce (PO) (Figure 3). The SeaSondes operate at a center frequency of 4.463 MHz and 25.734 kHz bandwidth. Lower frequencies allow for ranges close to 120 km at a spatial and angular resolution of 6 km and 5, respectively. Both the CB and PO stations operate since early 2015, with the CB antenna providing radial data since February 22, and the PO antenna since March 12 (Figure 4a). Measured antenna patterns at both sites provide for a correction in ideal (I) radial velocities due to potential interactions with other materials. Radial velocities obtained using measured antenna patterns will be referred to as measured (M) radials hereafter.

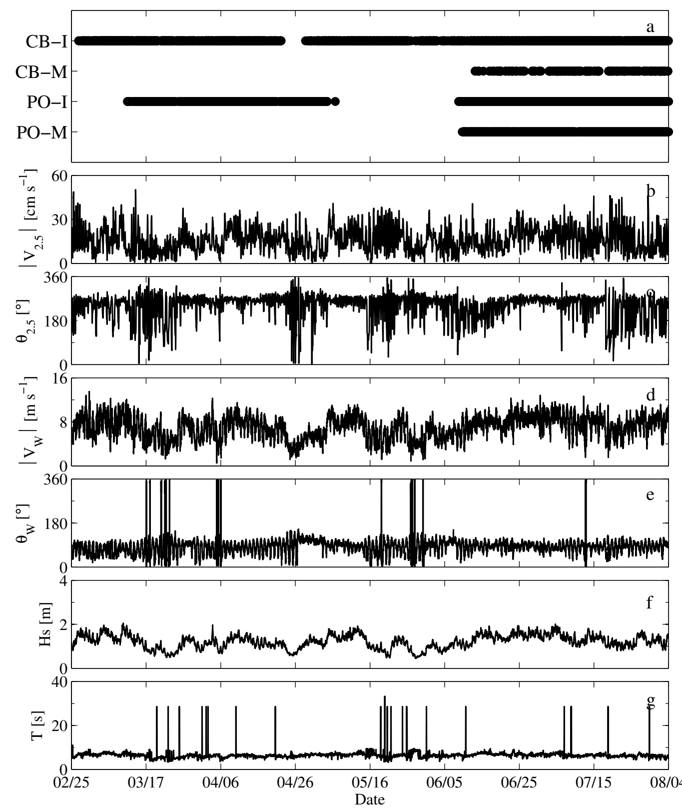

Fig. 4. (a) Data availability for Cabo Rojo ideal radials (CB-I), Cabo Rojo measured radials (CB-M), Ponce ideal radials (PO-I), and Ponce measured radials (PO-M). (b-c) Current speed and direction at 2.5 m of water depth as measured by the moored ADCP. (d-e) Wind speed and direction from the buoy's anemometer. (f-g) Significant wave height and dominant wave period, as resolved by the buoy's accelerometer.

C. Moored ADCP

Current velocities were resolved with a Nortek Aquadopp Z-Cell 600 kHz profiler, attached to CariCOOS' PR108 mooring. The oceanographic buoy is located southeast of Caja de Muertos island in 17 m of water depth. The ADCP sampled every 6 seconds and averaged over 8 minutes bursts. Current

TABLE I
SUMMARY OF STATISTICS FOR V_{HF}-V_{ADCP} COMPARISON.

	CB-I	CB-M	PO-I	PO-M
N	2499	287	2536	1306
Bearing	97.6°	97.2°	138.7°	139.0°
ΔV_{rms}*	17.1	27.3	11.4	12.9
ρ^2	0.24	0.07	0.46	0.34
Bias*	-7.87	-17.17	-5.75	-9.04
$m \pm \epsilon$	0.74 ± .03	0.51 ± .14	0.98 ± .03	0.80 ± .04
$b \pm \epsilon$	-4.83 ± .59	-11.68 ± 2.5	-5.67 ± .32	-8.31± .47

*cm s^{-1}

data were reported every hour for the entire length of the validation experiment. Wave and wind data were provided by an accelerometer and anemometer, respectively, both located within the buoy.

III. RESULTS

Radial velocities from HF (V_{HF}) were compared to the shallowest component of the buoy's ADCP current velocity in the direction of the HF radar (V_b) such that

$$V_b = \mathbf{V}_{2.5} \cdot \mathbf{i} \tag{1}$$

where $\mathbf{V}_{2.5}$ is the total velocity vector of the moored ADCP at 2.5 m of water depth, $(\cdot)$ corresponds to the dot product, and $\mathbf{i}$ is the unit vector pointing towards the radar from the mooring site. Both, ideal (I) and measured (M) radials were examined for both, the Cabo Rojo (CB) and Ponce (PO) sites. Given the abrupt change in bathymetry a few kilometers south of the mooring, only radials within 3 km from the mooring site were considered, resulting in sector bearings as shown in Table I (measured from the antenna to the sector in degrees from true North).

A. Time-domain analysis

Comparisons between V_{HF} and V_b were performed based on the squared of the correlation coefficient ρ^2, root-mean-square difference (ΔV_{rms}), bias, and coefficients of the least squares fits (Table I). The root-mean-square difference was computed following [6], with

$$\Delta V_{rms} = \left\{ \overline{\left[(V_{HF} - \overline{V}_{HF}) - (V_b - \overline{V}_b) \right]^2} \right\}^{1/2} \tag{2}$$

while velocity bias was calculated by subtracting $\overline{V}_b$ from $\overline{V}_{HF}$, where overbars indicate time averages. Least squares regression coefficients follow $V_{HF} = mV_b + b$, with standard error (ϵ) computed at the 90% confidence level.

Ponce HF radar data, especially measured radials, show a tendency towards more negative (southeast-directed) values (Figure 5 and 6). As shown by the scatter plot, V_{HF} is for the most part underestimated with respect to the 1:1 relationship. The same is true for the Cabo Rojo site (figures not shown), with biases reaching up to -17.17 cm s^{-1} (Table I). Please note that due to the different bearing, negative biases in the Cabo Rojo site represent a tendency toward higher eastward velocities. The discrepancy cannot be attributed to wind shear, since the wind was predominantly coming from the East during the sampling period (Figure 4e).

Nonetheless, Ponce radials show consistently the best comparisons with near-surface currents measured by the moored ADCP, as evidenced by the higher ρ^2 values, lower ΔV_{rms}, and least squares slopes closer to 1 (Table I). This is not surprising given that the Ponce antenna is located less than 20 km from the buoy, as opposed to almost 100 km, which is the case for the Cabo Rojo antenna.

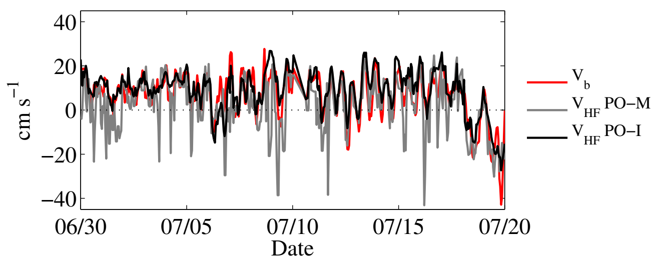

Fig. 5. Sample time series of Ponce ideal V_{HF} (black), Ponce measured V_{HF} (gray), and V_b (red) for a three-week period.

The statistics also consistently show that ideal radials compare better to moored data than measured radials for both, the Cabo Rojo and Ponce sites. This has been reported before in [7], and may be attributed to improper calibration and/or severe environmental conditions potentially affecting the hardware. Note that the number of data points available for comparison reduces significantly after measuring antenna patterns, as previously reported by [8] and others. For the case of Cabo Rojo, the sector number reduces almost one order of magnitude, and about half for the Ponce site, suggesting that the measured antenna pattern is rather strict for Cabo Rojo.

Summarizing the statistics, the consistently negative velocity biases and y-intercepts suggest a tendency of the HF radars to observe higher radial velocities in the direction away from the antenna, while the regression slope points at consistently lower magnitudes of V_{HF}. Except for CB-M, velocity differences are similar to those reported in the literature (see [6]). Overall, Ponce radials, especially ideal radials, show the best comparisons with the ADCP data.

B. Cross-spectral analysis

The power spectral density, as well as the coherence and phase spectra between V_{HF} and V_b were computed for three of the four sites. Both, Ponce ideal radials and ADCP, are able to detect diurnal and semidiurnal signals in their measured currents (Figure 7a). They are consistently coherent for frequencies lower than 0.1 hr^{-1}, and show phase differences with values very close to zero. A significant, yet low energy peak at the next harmonic (0.16 hr^{-1}) is also detected by the two sensors, and shows coherence and very low phase difference. Spectral analyses of Ponce measured radials and

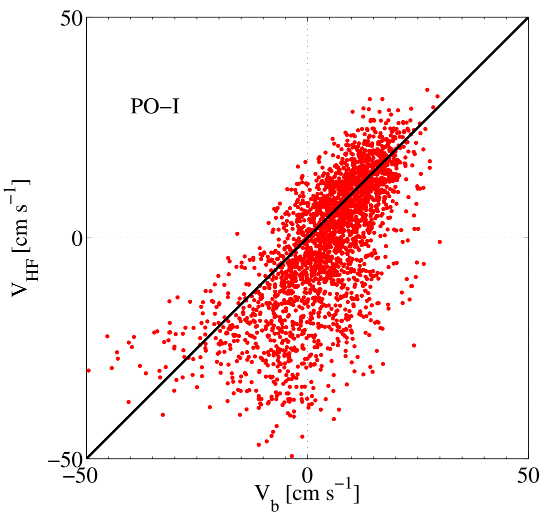

Fig. 6. Scatter plot of V_{HF} against V_b for Ponce ideals corresponding to the entire period of data collection. The solid black line indicates a 1:1 relationship.

Cabo Rojo ideal radials (figures not shown) suggest higher noise floors and inability to resolve peaks at frequencies other than the diurnal. Spectral analyses for Cabo Rojo measured radials were not performed due to the large amount of gaps in the data.

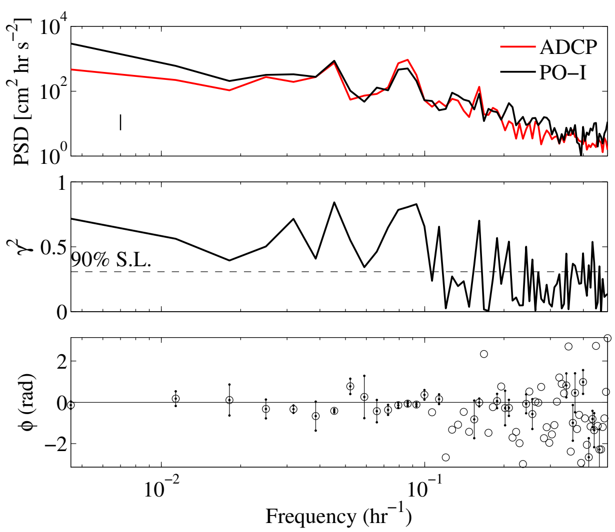

Fig. 7. (a) Power spectral density of V_{HF} and V_b based on Ponce ideal radials. Vertical line in the lower left corner indicates significance at the 90% level with 18 degrees of freedom. (b) Coherence squared spectrum between V_{HF} and V_b. (c) Phase spectrum between V_{HF} and V_b.

C. Drifter trajectories and PTM

Lagrangian data from the CariCOOS-CFMC drifter program was compared with radar-derived particle trajectories using a stochastic dynamic particle tracking model (PTM), which incorporates the random flight model discussed in [9]. Ideal radial data was processed using an equally spaced 6 km by 6 km grid, followed by a 5 km distance-weighted optimal interpolation. The signal variance and data error variance were set to 420 cm^2 s^{-2} and 66 cm^2 s^{-2}, respectively, in order to maintain the quality of total vector velocities [10]. Radial vectors exceeding the maximum geometric dilution of precision were also removed prior to processing [11]. Gridded data pertaining to March 31-April 4, 2015 was then used as input for the PTM, which consisted of 10 particles released at 17.884 N and -66.892 W, roughly 30 km south of Guanica, PR.

A qualitative comparison between radar-derived particle trajectories and a lagrangian drifter shows the HF radars overestimating a southward current near the point of release. Roughly two days after release, the westward current seems to dominate both, the drifter and PTM. By day four, the particle trajectories are considerably separated. While drifter trajectories may be slightly influenced by wind shear [12], this preliminary analysis suggests that radar-derived particle trajectories resemble drifter tracks fairly well for the first 1.5 days.

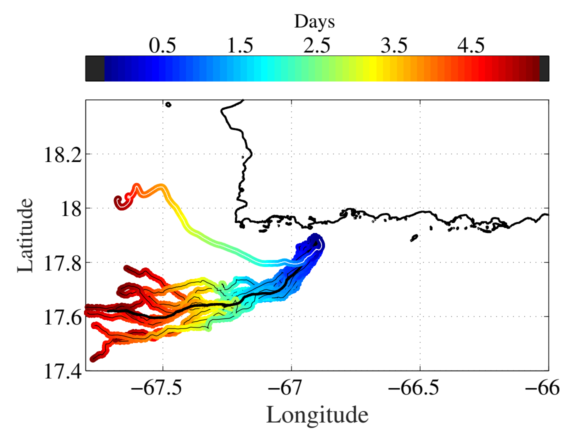

Fig. 8. Drifter trajectory (white), 10 PTM trajectories (black thin lines), and mean PTM trajectory (black thick line) for March 31-April 4, 2015. The colorbar indicates days from release.

IV. Summary and Concluding Remarks

Near-surface currents as resolved by HF radars were compared to ADCP and drifter data in order to assess the shoreward extent at which HF radars are able to depict surface currents potentially associated with MSEs interactions with littoral waters. Analysis in the time domain reveal better comparisons between the ADCP shallowest bin and HF ideal radials, especially for the antenna closest to the mooring site. The statistics also show that Cabo Rojo and Ponce radial velocities are slightly biased toward the East and Southeast, respectively. In the frequency domain, ideal radial data show less noise and ability to resolve the dominant spectral peaks at the site. The mean track of radar-derived particle trajectories closely resemble drifter data for the first 36 hours after release. While further comparisons including bearing offsets, as well as additional ADCP locations and drifters are in order, these analyses suggest that HF radars may be able to resolve near surface currents associated with MSE interactions with littoral waters. Our results suggests that for the current configuration ideal radial data be used, and antenna patterns be re-assesed and measured with more frequency.

ACKNOWLEDGMENTS

This effort is supported by CariCOOS through NOAA Integrated Ocean Observing System (IOOS), grant NA11NOS0120035. The CariCOOS-CFMC drifter program acknowledges funding from NOAA Coral Reef Conservation Program, grant FNA14NMF4410150 through the Caribbean Fisheries Management Council. We also appreciate technical support from Ethan Handel and the RUCOOL team.

REFERENCES

[1] R. Morrow and P.-Y. Le Traon, "Recent advances in observing mesoscale ocean dynamics with satellite altimetry," *Advances in Space Research*, vol. 50, no. 8, pp. 1062–1076, 2012.

[2] J. M. Morell, J. E. Corredor, and W. J. Merryfield, "Thermohaline staircases in a caribbean eddy and mechanisms for staircase formation," *Deep Sea Research Part II: Topical Studies in Oceanography*, vol. 53, no. 1, pp. 128–139, 2006.

[3] C. Cenedese, R. E. Todd, G. G. Gawarkiewicz, W. B. Owens, and A. Y. Shcherbina, "Offshore transport of shelf waters through interaction of vortices with a shelfbreak current," *Journal of Physical Oceanography*, vol. 43, no. 5, pp. 905–919, 2013.

[4] A. H. Chaudhuri, J. J. Bisagni, and A. Gangopadhyay, "Shelf water entrainment by gulf stream warm-core rings between 75 w and 50 w during 1978–1999," *Continental Shelf Research*, vol. 29, no. 2, pp. 393–406, 2009.

[5] E. Quinones, F. Garcia, M. Canals, J. M. Morell, C. J, and J. Lebron, "Offshore drifter deployment and tracking at the marine protected area off western puerto rico," poster presented at the 2015 CariCOOS General Assembly Meeting.

[6] B. M. Emery, L. Washburn, and J. A. Harlan, "Evaluating radial current measurements from codar high-frequency radars with moored current meters*," *Journal of Atmospheric and Oceanic Technology*, vol. 21, no. 8, pp. 1259–1271, 2004.

[7] P. Lorente, S. Piedracoba, and E. A. Fanjul, "Validation of high-frequency radar ocean surface current observations in the nw of the iberian peninsula," *Continental Shelf Research*, vol. 92, pp. 1–15, 2015.

[8] C. M. Halle and J. L. Largier, "Surface circulation downstream of the point arena upwelling center," *Continental Shelf Research*, vol. 31, no. 12, pp. 1260–1272, 2011.

[9] A. Griffa, "Applications of stochastic particle models to oceanographic problems," in *Stochastic modelling in physical oceanography*. Springer, 1996, pp. 113–140.

[10] J. Kohut, H. Roarty, E. Randall-Goodwin, S. Glenn, and C. S. Lichtenwalner, "Evaluation of two algorithms for a network of coastal hf radars in the mid-atlantic bight," *Ocean Dynamics*, vol. 62, no. 6, pp. 953–968, 2012.

[11] R. Chapman, L. Shay, H. Graber, J. Edson, A. Karachintsev, C. Trump, and D. Ross, "On the accuracy of hf radar surface current measurements: Intercomparisons with ship-based sensors," *Journal of Geophysical Research: Oceans (1978–2012)*, vol. 102, no. C8, pp. 18 737–18 748, 1997.

[12] R. Lumpkin, S. A. Grodsky, L. Centurioni, M.-H. Rio, J. A. Carton, and D. Lee, "Removing spurious low-frequency variability in drifter velocities," *Journal of Atmospheric and Oceanic Technology*, vol. 30, no. 2, pp. 353–360, 2013.